



Full Text View

[Volume 29, Issue 9 \(September 1999\)](#)

Journal of Physical Oceanography

Article: pp. 2462–2467 | [Abstract](#) | [PDF \(101K\)](#)

Fronts Formed by Obliquely Reflecting Internal Waves at a Sloping Boundary

S. A. Thorpe

School of Ocean and Earth Science, Southampton Oceanography Centre, Southampton, United Kingdom

(Manuscript received September 17, 1998, in final form February 24, 1999)

DOI: 10.1175/1520-0485(1999)029<2462:FFBORI>2.0.CO;2

ABSTRACT

A characteristic of internal waves reflecting from sloping boundaries is that they form fronts that travel with the component of the phase speed of the waves up the boundary. The strength of the fronts is assessed by estimating the magnitude of nonlinear terms leading to the asymmetry of density gradients at the slope when waves travelling in a fluid of uniform buoyancy frequency are at nonnormal, or oblique, incidence to the slope. Strong nonlinearities, indicating fronts, are found for both supercritical ($\beta > \alpha$) and subcritical ($\beta < \alpha$) waves near critical slopes where the inclination of the boundary to the horizontal, α , matches that of the wave group velocity β . They are also found for subcritical waves when β is near $\sin^{-1}[(\sin\alpha)/2]$. Fronts become weaker as the angle at which the wave approaches the slope, the azimuth or incident angle, increases from zero (i.e., when waves are nonnormal), but not significantly so until this angle exceeds 30° .

1. Introduction

There is much interest in the processes that lead to mixing at, or near, the sloping boundaries of oceans and lakes. This is prompted by observations of enhanced rates of dissipation near the Mid-Atlantic Ridge bounding the eastern side of the Brazil Basin ([Polzin et al. 1997](#)), near seamounts ([Toole et al. 1997](#); [Eriksen. 1998](#)), and near lake or reservoir boundaries ([Imberger and Ivey 1991, 1993](#)), as well as by the higher rates of vertical diffusion of tracers that are found in tracer studies near slopes ([Ledwell and Watson 1991](#); [Ledwell and Hickey 1995](#); [Ledwell and Bratkovich 1995](#)). It is known that internal waves reflecting from sloping boundaries may produce reflected waves that are steeper, produce greater shear, and have smaller characteristic Richardson numbers than the incident waves ([Eriksen 1982, 1985](#)), particularly when the slope of the boundary is near-critical, that is, when $\sin\alpha$ is approximately equal to σ/N ($=\sin\beta$), where α is the inclination of the sloping boundary to the horizontal, σ is the wave frequency, and N is the buoyancy frequency. A characteristic of waves reflecting from sloping boundaries—at least when they approach “normally,” that is, their group velocity vector lies in a vertical plane that intersects the sloping boundary along a line of greatest slope—is that

Table of Contents:

- [Introduction](#)
- [Analysis](#)
- [Results](#)
- [Conclusions](#)
- [REFERENCES](#)
- [APPENDIX](#)
- [FIGURES](#)

Options:

- [Create Reference](#)
- [Email this Article](#)
- [Add to MyArchive](#)
- [Search AMS Glossary](#)

Search CrossRef for:

- [Articles Citing This Article](#)

Search Google Scholar for:

- [S. A. Thorpe](#)

they produce regions of enhanced density gradient, or *fronts*, which move up the slope with the advancing wave phase. Such fronts produced by waves at normal incidence have been observed in laboratory experiments (Thorpe 1987), and they have been studied analytically (Thorpe 1992) and are found in numerical simulations (Slinn and Riley 1998). They are often associated with the onset of turbulence and mixing typical of that in gravity currents (Ivey and Nokes 1989; Thorpe et al. 1991; Taylor 1993; Slinn and Riley 1998).

While fronts are also evident in measurements within a few meters of oceanic (Thorpe 1992) and lake (Lemmin et al. 1998) slopes, the orientation (relative to the boundary contours) of the incident waves causing them has not been observed. Recent laboratory experiments (Dunkerton et al. 1998) with azimuth angles of about 18° have, however, demonstrated that fronts *can* occur when internal waves approach a slope nonnormally, or “obliquely.” The purpose of this note is to examine analytically what effect nonnormal incidence may have on the steepening of waves at sloping boundaries and, in particular, to see whether steeper waves may occur at the boundary if reflection is nonnormal but when the characteristics of the incident waves (i.e., β and the wave steepness) are unchanged. The effects of wave breaking and alongslope current generation at the slope (Thorpe 1999a) are ignored.

2. Analysis

a. The steepening of waves on the sloping boundary

The analytical method follows that described by Thorpe (1987, 1992). Rotation is neglected ($f = 0$). Nonlinear wave components with frequency 2σ and wavenumber components ($2k$, $2l$) in the x and y directions, respectively up and along the plane slope, are generated by the interaction of an incident wave with wavenumber (k , l , m_I) (with the z direction upward, normal to the slope) and frequency (σ) and a (first order) reflected wave with components (k , l , m_R) and conserved frequency σ . [An exact solution is available for the incident wave. The interactions considered here are “sum” interactions; the “difference” interactions generate steady currents and are discussed by Thorpe (1997).] The wavenumbers normal to the slope are $m_I = -(k/\gamma)(s_\alpha c_\alpha - r s_\beta c_\beta)$ and $m_R = -(k/\gamma)(s_\alpha c_\alpha + r s_\beta c_\beta)$, which satisfy the dispersion relation $\sigma^2 = N^2 s_\beta^2$, where $s_\alpha = \sin\alpha$, $c_\beta = \cos\beta$, etc., $\gamma = s_\beta^2 - s_\alpha^2$, and $r = [1 + l^2\gamma/(k^2 s_\beta^2)]^{1/2}$. The velocity and density perturbations of the incident and first-order reflected waves are given in appendix B (from Thorpe 1997). Correct to first order the density on the slope at $z = 0$ is $\rho_0[1 - (N^2 s_\alpha/g)x] + \rho_1$, where

$$\rho_1 = -(2\rho_0 a k s_\alpha s_\beta c_\beta N^2/g\sigma\gamma) \sin(kx + ly - \sigma t), = \rho_0 s q_1 \sin(kx + ly - \sigma t), (1)$$

say, and $ak = -\sigma s \gamma^2 / [k s_\beta c_\beta (s_\alpha c_\beta - r s_\beta c_\alpha)^2]$, where s is the steepness of the incident wave, an ordering parameter, and ρ_0 is a reference density.

Second-order terms are found by reiteration, using the first-order terms to estimate product terms in the equations of motion and density conservation, and then solving these subject to the condition that the velocity normal to the slope is zero on the slope at $z = 0$, as described in appendix C. The second-order density perturbation, periodic in x , y , and t , is

$$\rho_2 = \rho_0 s^2 q_2 \sin[2(kx + ly - \sigma t)], (2)$$

at $z = 0$, where q_2 is a function of α , β , and θ .

Using (1) and (2), the total density perturbation on the sloping boundary, which varies periodically in x , y and t , is $\rho = \rho_0 [s q_1 \sin(kx + ly - \sigma t) + s^2 q_2 \sin[2(kx + ly - \sigma t)]]$. Values of q_1 and q_2 are found numerically from the analytical solutions. The term q_2 is < 0 for the supercritical waves with $\alpha/\beta < 1$. The contribution of the second-order terms with $q_2 < 0$ for α near β results in an asymmetry in the density, with a relatively steep fall in density at phase $kx + ly - \sigma t = 2n\pi$, ($n = 1, 2, 3, \dots$), and with gradual recovery in between. Correspondingly at fixed times t , an enhanced density rise is found at positions $kx + ly = 2n\pi + \sigma t$, and this advances with the wave phase speed as t increases. For subcritical waves with $1 < \alpha/\beta < 2$, $q_2 > 0$, and the second-order terms again result in an enhanced rise in density, but now at $kx + ly - \sigma t = (2n + 1)\pi$, ($n = 1, 2, 3, \dots$).

b. Constant phase lines on the slope

The orientation of fronts on the sloping boundary is given by the lines of constant wave phase. Figure 1 shows how a

constant phase surface of an incident wave, inclined at angle β to the horizontal, meets a plane boundary inclined at angle α to the horizontal. The intersection is along a line AB. The wave group velocity is at right angles to the phase velocity (Phillips 1966). The latter is normal to the surface of constant phase, so therefore the group velocity lies in the constant phase plane and is in a direction, AE down its steepest slope. The line AB is a constant phase line on the slope for both the incident and reflected wave. (AB therefore also lies in a constant phase plane of the reflected wave that, since the wave frequency and therefore the inclination β are conserved, is also inclined at angle β to the horizontal.) It is shown by simple geometry in appendix A that AB makes an angle Φ with line AC of greatest slope on the boundary given by

$$\Phi = \tan^{-1}(\cos\alpha \cot\theta + \cot\beta \csc\theta \sin\alpha), (3)$$

where θ is the angle that BE, the line of intersection of the constant phase plane and a horizontal plane, makes with BC a horizontal line in the plane of the slope. The angle θ is also the angle between the projection of the group velocity (direction AE) onto the horizontal (DE) and the projection of a line of greatest slope (e.g., AC) onto the horizontal (direction CD). The angle θ is therefore the angle of incidence of the internal wave to the slope measured in a horizontal plane. From (3), $\Phi = \pi/2$ when the angle of incidence, θ , = 0. At $\theta = \pi/2$, $\Phi = \tan^{-1}(\sin\alpha \cot\beta)$, but, when $\Phi = 0$, it is found that

$$\theta = -\cos^{-1}(\tan\alpha \cot\beta). (4)$$

There are no solutions to (4) if the waves are subcritical; that is, when $\alpha > \beta$. In that case the direction of the wave group velocity eventually becomes tangential to the slope as θ increases, and at larger θ there are no waves approaching the slope. This is illustrated in Fig. 1b. The slope is again the plane ABC. The incident angle, θ , is that between the directions CD and the projection of the group velocity vector onto the horizontal plane, BCD. Three cases are illustrated: (i) $\theta = 0$, when EB represents the group velocity vector. As θ increases, the vector rotates about the vertical line BG. (ii) At $\theta = \pi/2$ it becomes FB, where BC is its projection onto the horizontal. As θ increases further, the vector (keeping β constant) eventually lies parallel to the slope along the line AB at $\theta = \theta_c$, say (case iii). Further increase in θ places the vector below the sloping boundary; no waves can exist for such θ . The limiting value is $\theta_c = \pi/2 + \text{angle CBD}$, and since $\sin(\text{CBD}) = \text{CD}/\text{BD} = (\text{AD} \cot\alpha)/(\text{AD} \cot\beta)$, so

$$\cos\theta_c = -\tan\beta \cot\alpha. (5)$$



Relations (3)–(5) are used in section 3.


3. Results

The intensity, or strength, of the density “fronts” depends on the relative steepening produced by the second-order terms and hence on the ratio $R = q_2/q_1$. This determines both the asymmetry of spatial gradients, found by differentiating ρ with respect to x or y , and the temporal gradients found by time differentiation, both of which introduce a multiplicative factor 2 to the ratio of the second to the first-order contributions. The variation of R with α/β at $\alpha = 5^\circ$ for various incident angles θ is shown in Fig. 2a, for $0.5 < \alpha/\beta < 1$, while the variation of $-R$ (>0) is shown in Fig. 2b for $1 < \alpha/\beta < 2$. Here $|R|$ decreases as θ increases from 0 to 90° . Large values are found near the critical slope where $\alpha = \beta$, evidence of the dominance of nonlinear terms and the formation of fronts. Values of $|R|$ greater than 10, those for which the size of the second-order terms would match the first-order terms for an incident wave steepness of $s = 0.1$, are found in $0.84 < \alpha/\beta < 1.28$ when $\theta = 0^\circ$, but only in the narrower range $0.9 < \alpha/\beta < 1.12$ when $\theta = 60^\circ$.

Large values of $|R|$ are also evident in Fig. 2b as α/β approaches a value of near 2. These are a consequence of a singularity of the interaction component with wavenumber ($2k$, $2l$, m_2) and frequency 2σ . The formula for m_2 is given in appendix C, (C4). This forced component corresponds to a wave inclined at angle $\sin^{-1}(2\sigma/N)$ to the horizontal plane, which has the same inclination as the slope. It is therefore “critical,” with m_2 tending to infinity (zero wavenumber), when $\alpha = \sin^{-1}(2\sigma/N)$ or, since $\sigma/N = \sin\beta$, when $\sin\alpha/\sin\beta = 2$. The angle $\alpha = 5^\circ$ in Fig. 2, and so these critical conditions occur when $\beta = 2.498^\circ$, or $\alpha/\beta = 2.002$. It is particularly noticeable at the larger values of θ that the width of the range in α/β for which $|R|$ exceeds some given value is smaller at $\alpha/\beta = 2$ than at $\alpha/\beta = 1$; that is, at fixed β , the range of boundary slopes, α , which produce comparable $|R|$ is greater near $\alpha = \beta$ than near $\alpha = 2\beta$. It may be expected that when higher order terms are included, new singularities will occur and, at the n th order, will be found when $\sin\alpha/\sin\beta = n$.





Figure 3 shows how R varies with θ at fixed values of α/β . For supercritical waves (Fig. 3a), R decreases with θ , tending to zero when θ is near 150° . The orientation of the regions of enhanced density is determined by the intersection of the constant phase planes in the internal wave field and the sloping boundary or by the angle Φ defined by (3). From (2) it is found that the angle Φ is zero when $\theta = 154.2^\circ$ (or 153.1°) for $\alpha = 5^\circ$ (or 20°) and $\beta = 5.55^\circ$ (22.2°), respectively,

corresponding to the curves in [Fig. 3a](#) . These angles θ are where the front, if one existed, would be directly up and down the slope but, as seen in [Fig. 3a](#) , is where $R = 0$, so there is no steepening or tendency to form a front. Here R increases as θ increases between 160° and 180° (the limit in which the waves are propagating at normal incidence down the slope) and here the $\alpha = 5^\circ$ and $\alpha = 20^\circ$ curves are almost identical.

A similar trend of $|R|$ is found for subcritical waves ([Fig. 3b](#) ) as θ increases from 0° to about 150° where $|R|$ again tends to zero. This is where the incident subcritical waves become parallel to the boundary at $\theta = \theta_c$. Using [\(5\)](#) it is found that at $\alpha = 5^\circ$ (or 20°) and $\beta = 4.55^\circ$ (18.2°), $\theta_c = 155.3^\circ$ (or 154.5°), respectively. No waves exist for greater θ .

4. Conclusions

The principal conclusions are that

1. when the ratio α/β of the slope angle α to the wave angle β is kept constant, and the wave steepness s is also unchanged, the fronts formed by the process of internal wave reflection from a plane boundary will become weaker as the angle of wave incidence, θ , defined in [section 2a](#), increases from zero, but not significantly so until θ exceeds about 30° (see [Fig. 3](#) ). Fronts will strengthen as θ approaches 180° ([Fig. 3](#) ). The trends are not very sensitive to the choice of the inclination of the boundary α if less than about 20° .
2. Fronts become stronger as α approaches the critical slope β . Fronts are expected to form over a broader range of values α/β as θ approaches 0° or 180° ([Fig. 2](#) ).
3. Subcritical waves with wave angle β near $\sin^{-1}[(\sin\alpha)/n]$, $n = 2, 3, \dots$, may also form fronts, although over ranges of α/β which probably become relatively narrower as n increases. This is a consequence of the interaction between the incident and reflected components generating harmonics, $n\sigma$, which themselves become critical (e.g., see [Fig. 2b](#) ).

The conclusions are subject to reservations concerning the neglect of higher-order terms in wave steepness s and the assumptions inherent in the methodology, particularly that the second-order terms are significantly less than the first, clearly invalid when sR is large. The calculations provide at best a strong indicator of the relative conditions favorable for the formation of fronts, which laboratory experiments have shown *do* form when $\theta = 0^\circ$ ([Thorpe 1987](#)) and 18° ([Dunkerton et al. 1998](#)). Further study, perhaps by further laboratory work and numerical studies, is warranted.

The solutions for the density perturbation may be periodic in z , suggesting that high density gradients form above $z = 0$. While this may be so in the solutions, in reality the tendency for internal waves to arrive irregularly or in groups ([Thorpe 1999b](#)) means that the incident and reflected components overlap in space only close to $z = 0$, and interactions at greater distance may be less significant.

The formation of such fronts in the ocean will be affected by the coexistence of many internal waves with a broad spectrum of frequencies, and hence a wide range of β , and coming from a range of directions, θ . Fronts are likely to be formed only by the largest waves present locally at a given time, and those with near-critical frequencies traveling almost normal (i.e., within $\pm 30^\circ$) to the boundary. The formation of fronts, and attendant wave breaking and mixing, perhaps with the generation of alongslope currents ([Thorpe 1999a](#)), will change the density and velocity fields through which higher wavenumber waves travel, producing refraction and caustics and promoting conditions akin to surf on the sea shore.

Acknowledgments

I am grateful to Dr. Tim Dunkerton and his colleagues for allowing me to refer to their paper prior to its publication.

REFERENCES

Dunkerton, T. J., D. P. Delisi, and M.-P. Lelong, 1998: Alongslope current generated by obliquely incident internal gravity waves. *Geophys. Res. Lett.*, **25**, 3871–3874..

Eriksen, C. C., 1982: Observations of internal wave reflection off sloping bottoms. *J. Geophys. Res.*, **87**, 525–538..

—, 1985: Implications of ocean bottom reflection for internal wave spectra and mixing. *J. Phys. Oceanogr.*, **15**, 1145–1156.. [Find this article online](#)

— ,1998: Internal wave reflection and mixing at Fieberling Guyot. *J. Geophys. Res.*, **103**, 2977–2994..

Imberger, J., and G. N. Ivey, 1991: On the nature of turbulence in a stratified fluid. *J. Phys. Oceanogr.*, **21**, 659–680.. [Find this article online](#)

— ,and — ,1993: Boundary mixing in stratified reservoirs. *J. Fluid Mech.*, **248**, 477–491..

Ivey, G. N., and R. I. Nokes, 1989: Vertical mixing due to breaking of critical internal waves on sloping boundaries. *J. Fluid Mech.*, **204**, 479–500..

Ledwell, J. R., and A. J. Watson, 1991: The Santa Monica Basin Tracer Experiment; A study of diapycnal and isopycnal mixing. *J. Geophys. Res.*, **96**, 8695–8718..

— ,and A. Bratkovich, 1995: A tracer study of mixing in the Santa Cruz Basin. *J. Geophys. Res.*, **100**, 20 681–20 704..

— ,and B. M. Hickey, 1995: Evidence of enhanced boundary mixing in the Santa Monica Basin. *J. Geophys. Res.*, **100**, 20 665–20 679..

Lemmin, U., R. Jiang, and S. A. Thorpe, 1998: Finestructure dynamics of stratified waters near a sloping boundary of a lake. *Physical Processes in Lakes and Oceans*. J. Imberger, Ed., *AGU Coastal and Estuarine Studies*, Vol. 54, Amer. Geophys. Union, 461–474..

Phillips, O. M., 1966: *The Dynamics of the Upper Ocean*. Cambridge University Press, 261 pp..

Polzin, K. L., J. M. Toole, J. R. Ledwell, and R. W. Schmitt, 1997: Spatial variability of turbulent mixing in the abyssal ocean. *Science*, **276**, 93–96..

Slinn, D. N., and J. J. Riley, 1998: Turbulent dynamics of a critically reflecting internal gravity wave. *Theor. Comput. Fluid Dyn.*, **11**, 281–304..

Taylor, J. R., 1993: Turbulence and mixing in the boundary layer generated by shoaling internal waves. *Dyn. Atmos. Oceans*, **19**, 233–258..

Thorpe, S. A., 1987: On the reflection of a train of finite amplitude internal waves from a uniform slope. *J. Fluid Mech.*, **178**, 279–302..

— ,1992: Thermal fronts caused by internal gravity waves reflecting from a slope. *J. Phys. Oceanogr.*, **22**, 105–108.. [Find this article online](#)

— ,1997: On the interactions of internal waves reflecting from slopes. *J. Phys. Oceanogr.*, **27**, 2072–2078.. [Find this article online](#)

— ,1999a: The generation of along-slope currents by breaking internal waves. *J. Phys. Oceanogr.*, **29**, 29–38.. [Find this article online](#)


— ,1999b: On internal wave groups. *J. Phys. Oceanogr.*, **29**, 1085–1095.. [Find this article online](#)

— ,M. Cure, and M. White, 1991: The skewness of temperature derivatives in oceanic boundary layers. *J. Phys. Oceanogr.*, **21**, 428–433.. [Find this article online](#)

Toole, J. M., R. W. Schmitt, and K. L. Polzin, 1997: Near-bottom mixing above the flanks of a midlatitude seamount. *J. Geophys. Res.*, **102**, 947–959..

APPENDIX A

5. The Orientation of Constant Phase Lines

[Figure 1](#)  shows a constant phase plane of the incident internal wave and its line of intersection, AB, with the sloping boundary. AC is a line of greatest slope on the boundary that makes an angle α with the horizontal plane BCD, where D is vertically below A. The constant phase surface makes an angle $AED = \beta$ with the horizontal plane, and the line AB makes an angle ϕ with AC. This angle ϕ defines the orientation of constant wave phase lines on the slope. The angle θ defines the inclination of the incident wave to the slope. When θ is zero, the wave is normally incident and the incident and reflected wave field becomes two-dimensional. When $\theta = \pi/2$, the incident wave travels parallel to the slope.

The angle ϕ can be found in terms of other angles as follows. Since angle $EDA = \pi/2$, $ED = AD \cot\beta$ and since angle $EFD = \theta$, $FD = AD \cot\beta \csc\theta$. Since angle $ADC = \pi/2$, $CD = AD \cot\alpha$. Since FG is parallel and equal to DC, $BG = FG \cot\theta = AD \cot\alpha \cot\theta$. Hence $\tan\phi = BC/AC = (BG + GC)/AD \csc\alpha = (BG + FD)/AD \sin\alpha = (\cot\alpha \cot\theta + \cot\beta \csc\theta) \sin\alpha = \cos\alpha$

APPENDIX B

6. First-Order Solution

Exact wave solutions of the equations of motion and density conservation can be found in a fluid in a mean state of rest and with uniform buoyancy frequency, N . The equations of motion in a tilted frame of reference are given by [Thorpe \(1997\)](#) appendix a). The solutions for the three (u, \mathbf{v}, w) components of velocity in the x, y, z frame of reference and for the density perturbation ρ for the incident and reflected waves, which satisfy the boundary condition $w_I + w_R = 0$ (subscripts I and R stand for the incident and reflected wave, respectively) at the sloping plane $z = 0$, are $u_I = (ak/\gamma)(s_\beta c_\beta - rs_\alpha c_\alpha)c_P$, $\mathbf{v}_I = (alc_\beta/s_\beta)c_P$, $w_I = -akrc_P$, $\rho_I = -(aks_\beta N^2 \rho_0/g\sigma\gamma)(s_\alpha c_\beta - rs_\beta c_\alpha)s_I$; $u_R = (ak/\gamma)(s_\beta c_\beta + rs_\alpha c_\alpha)c_R$, $\mathbf{v}_R = (alc_\beta/s_\beta)c_R$, $w_R = akrc_R$, $\rho_R = -(aks_\beta N^2 \rho_0/g\sigma\gamma)(s_\alpha c_\beta + rs_\beta c_\alpha)s_R$ ([Thorpe 1997](#)).

Here $s_I = \sin(kx + ly + m_I z - \sigma t)$, $c_R = \cos(kx + ly + m_R z - \sigma t)$, etc., and $ak = -\sigma\gamma^2/[ks_\beta c_\beta(s_\alpha c_\beta - rs_\beta c_\alpha)^2]$ where s is the incident wave steepness Am ; A is the amplitude of the incident internal wave with vertical wavenumber $m = k_I s_\alpha + m_I c_\alpha$. The steepness is a crucial measure of the waves, isopycnals being vertical in the internal wave field if $s = 1$ ([Thorpe 1987](#)). The first-order density perturbation on the slope is $(\rho_I + \rho_R)$ at $z = 0$, and is given by [\(1\)](#).

APPENDIX C

7. Second-Order Solution

The equations for the second-order velocity (u_2, \mathbf{v}_2, w_2) and density ρ_2 components can be reduced to two equations for w_2 and ρ_2 by elimination of u_2 and \mathbf{v}_2 :

$$\begin{aligned} & [\partial^3/\partial t^2 \partial z + N^2 s_\alpha (s_\alpha \partial/\partial z - c_\alpha \partial/\partial x)] \rho_2 \\ & - (N^2 \rho_0/g) \partial/\partial t [s_\alpha \partial/\partial x + c_\alpha \partial/\partial z] w_2 \\ & = -\partial^2 I_4/\partial t \partial z + (N^2 \rho_0 s_\alpha/g) (\partial I_3/\partial x - \partial I_1/\partial z), \quad (\text{C1a}) \end{aligned}$$

$$\begin{aligned} & \partial^2 \nabla^2 w_2/\partial t \partial x + (g/\rho_0) \partial/\partial x [c_\alpha (\partial^2/\partial x^2 + \partial^2/\partial y^2) - s_\alpha \partial^2/\partial x \partial z] \rho_2 \\ & = -(\partial^2/\partial x^2 + \partial^2/\partial y^2) (\partial I_3/\partial x - \partial I_1/\partial z) \\ & + \partial^2/\partial y \partial z (\partial I_2/\partial x - \partial I_1/\partial y), \quad (\text{C1b}) \end{aligned}$$

where $\nabla^2 = \partial^2/\partial x^2 + \partial^2/\partial y^2 + \partial^2/\partial z^2$, and $I_1 = \mathcal{F}_I(u_R) + \mathcal{F}_R(u_I)$ with the operator $\mathcal{F}_I = u \partial/\partial x + \mathbf{v} \partial/\partial y + w \partial/\partial z$; \mathcal{F}_R is similarly defined, and, I_2, I_3 , and I_4 are found by substituting the incident and reflected components \mathbf{v}, w , and p , respectively, defined in appendix B. Since the incident and reflected wave solutions are exact, all the I, I and R, R product terms vanish identically leaving only the I, R products. The terms in ρ_2 in [\(C1a\)](#) and [\(C1b\)](#) are eliminated to give an equation for w_2 in terms of the products of derivatives of the first-order terms. This has the solution

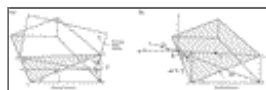
$$w_2 = W_1 \{ \cos[2kx + 2ly + (m_I + m_R)z - 2\sigma t] - \cos[2kx + 2ly + m_2 z - 2\sigma t] \}, (\text{C2})$$

which satisfies $w_2 = 0$ at $z = 0$, where W_1 is a function of α, β , and θ and is proportional to $s^2(\sigma/k)$. Here

$$m_2 = -2k[s_\alpha c_\alpha + \{(1-4s_\beta^2)[4s_\beta^2 + (l/k)^2(4s_\beta^2 - s_\alpha^2)]\}^{1/2}] \div (4s_\beta^2 - s_\alpha^2). \quad (C3)$$

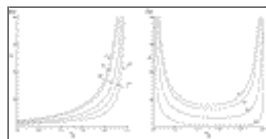
The solution w_2 is substituted into (C1b) to give an equation for ρ_2 . This is integrated to give second-order density terms periodic in x , y and t : $-\rho_2 = \Pi_1 \sin[2kx + 2ly + (m_I + m_R)z - 2\sigma t] + \Pi_2 \sin[2kx + 2ly + m_2 z - 2\sigma t]$, where Π_1 and Π_2 are easily calculated, but long, analytical functions of α , β , and θ , and are proportional to $s^2 \rho_0$. There are also second-order density terms independent of x, y and t , but which are sinusoidal in z (Thorpe 1987); however, these do not contribute to the density variations *along* the slope with which we are concerned here. The x, y, t periodic second-order density term can be written $\rho_2 = \rho_0 s^2 q_2 \sin[2(kx + ly - \sigma t)]$ at $z = 0$.

Figures



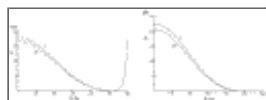
[Click on thumbnail for full-sized image.](#)

Fig. 1. (a) A diagram defining the notation and showing a constant phase plane of an internal wave and its intersection with an inclined plane forming a boundary to the fluid. The constant phase plane is inclined at an angle β to the horizontal and meets the plane boundary ABGC (stippled), inclined at angle α to the horizontal, in the line AB. The line AE, marked c_g , is in the direction of the group velocity. (b) A diagram showing how, as the incident angle θ increases, the internal wave group velocity vector c_g eventually becomes parallel to the sloping boundary ABC along the line AB. Shown are (i), $\theta = 0$; (ii), $\theta = \pi/2$; and (iii), the eventual limiting direction. The line marked $\theta = 0$ is parallel to CD and is the projection of EP onto the horizontal plane BCD.



[Click on thumbnail for full-sized image.](#)

Fig. 2. The variation of the ratio R of second- and first-order density terms with α/β for $\alpha = 5^\circ$ at various incident angles θ indicated on the graph, for (a) supercritical waves, $0.5 < \alpha/\beta < 1.0$, and (b) with $-R$, subcritical waves, $1.0 < \alpha/\beta < 2.0$.



[Click on thumbnail for full-sized image.](#)

Fig. 3. The variation of the ratio R with θ when $\alpha = 5^\circ$ and 20° and when (a) waves are supercritical with $\alpha/\beta = 0.9$ and (b) waves are subcritical with $\alpha/\beta = 1.1$.

Corresponding author address: Dr. S. A. Thorpe, Department of Oceanography, University of Southampton, Southampton Oceanography Centre, European Way, Southampton SO14 3ZH, United Kingdom.

E-mail: sxt@socnet.soc.soton.ac.uk

top ▲

